

## Cluster ionization via two-plasmon excitation

G. F. Bertsch,<sup>1</sup> N. Van Giai,<sup>2</sup> and N. Vinh Mau<sup>2</sup>

<sup>1</sup>*Department of Physics and Institute for Nuclear Theory, Box 351560, University of Washington, Seattle, Washington 98195*

<sup>2</sup>*Groupe de Physique Théorique, Institut de Physique Nucléaire, 91406 Orsay Cedex, France*

(Received 12 January 1999; revised manuscript received 15 October 1999; published 16 February 2000)

We calculate the two-photon ionization of clusters for photon energies near the surface plasmon resonance. The plasmon is described in a schematic jellium-RPA model assuming a separable residual interaction between electrons determined so that the plasmon energy is reproduced. The ionization rate of a double plasmon excitation is calculated perturbatively. In  $\text{Na}_{93}^+$  clusters we find an ionization rate of the order of at most  $0.05\text{--}0.10\text{ fs}^{-1}$ . This rate is used to determine the ionization probability in an external field in terms of the number of absorbed photon pairs and the duration of the field. We discuss the dependence of the results on the choice of our empirical separable force. The number of emitted electrons per pair of absorbed photons is found to be small, in the range  $10^{-5}$  to  $10^{-3}$ .

PACS number(s): 36.40.Vz, 61.46.+w

### I. INTRODUCTION

The electromagnetic response of alkali metal clusters shows a very strong surface plasmon resonance [1], but the interactions of the plasmon with other degrees of freedom are not well understood. One interesting question is the nonlinearities associated with multiple plasmon excitations—how weakly do they interact with each other? Some physical processes can be sensitive to nonlinearities; for example, ionization may be energetically impossible for individual plasmons but allowed for states with multiple plasmon excitations and therefore, ionization rates may depend on the degree of nonlinearity. Recently an experiment was reported observing the ionization probability with different photon field durations [2]. The photon energy was such that ionization is energetically possible only if at least two photons are absorbed. In this work we ask whether the observed ionization can be interpreted as a direct electron emission by a two-plasmon state within a simple theory based on the jellium model of the electronic structure. Of course, there may be other processes leading also to ionization but they are outside the scope of the present study.

We will use standard many-body perturbation theory, describing the surface plasmon in RPA as a particle-hole excitation. The plasmon description and details of the jellium model are given in Sec. II below where we present a semi-analytic approximation which leads to more transparent expressions for the physical quantities. Our calculation may be viewed as an approximation to time-dependent local density approximation (TDLDA), in which the electron dynamics is treated entirely by a common potential field. The TDLDA has been well developed for the high-field response of atoms [3–5], and is now being applied to sodium clusters [6]. Unfortunately, the full TDLDA is computationally difficult and rather opaque, in contrast to the perturbative approach that allows important quantities to be calculated directly.

From the point of view of surface plasmon dynamics, a very important quantity is the ionization rate of a two-plasmon excited state. Haberland *et al.* [2] interpreted their measurements under the assumption that this rate is fast on a time scale of 10 fs, and we wish to see whether that can be

justified theoretically. The two-plasmon ionization rate is calculated in Sec. III. In Sec. IV we use the ionization rate of the previous section to estimate the number of emitted electrons to allow a more direct comparison with experiments.

### II. THE ELECTRONIC STRUCTURE MODEL

In this section we discuss the Hamiltonian model and the treatment of the surface plasmon for the  $\text{Na}_{93}^+$  cluster. We will need single-electron wave functions and energies, which we calculate as follows. We first obtained the solution of the self-consistent jellium model using the computer code JELLYRPA [7]. The jellium background charge is assumed to be uniform in a sphere of radius  $R=r_s N^{1/3}$ . Here  $r_s=3.93$  a.u. corresponds to density of charge equal to the bulk density of atoms in sodium metal. For practical convenience we choose to replace the self-consistent potential by a fitted potential of Woods-Saxon shape:

$$V(r) = \frac{-V_0}{1 + e^{(r-R_0)/a}} - V_c(r), \quad (1)$$

whose parameters are  $V_0=5.71$  eV,  $R_0=10.548$  Å, and  $a=0.635$  Å. In Eq. (1)  $V_c(r)$  is a Coulomb field associated with the positive charge distributed uniformly in the jellium sphere,

$$V_c(r) = \frac{e^2}{r}, \quad r > N^{1/3} r_s, \\ = \frac{e^2}{R} \left( \frac{3}{2} - \frac{r^2}{2R^2} \right), \quad r < N^{1/3} r_s. \quad (2)$$

In Fig. 1 are displayed the single-electron spectra of the original self-consistent potential and of the fitted one. The corresponding energy levels of the two potentials are within 0.2 eV which is certainly enough for the accuracy of the jellium model. We find that the cluster has an ionization potential of 4.5 eV. Under the conditions of the experiment [2] using photons of 3.1 eV, two photons are required for ionization on energetic ground.

The RPA surface plasmon might also be calculated numerically with the code JELLYRPA. However, in order to have

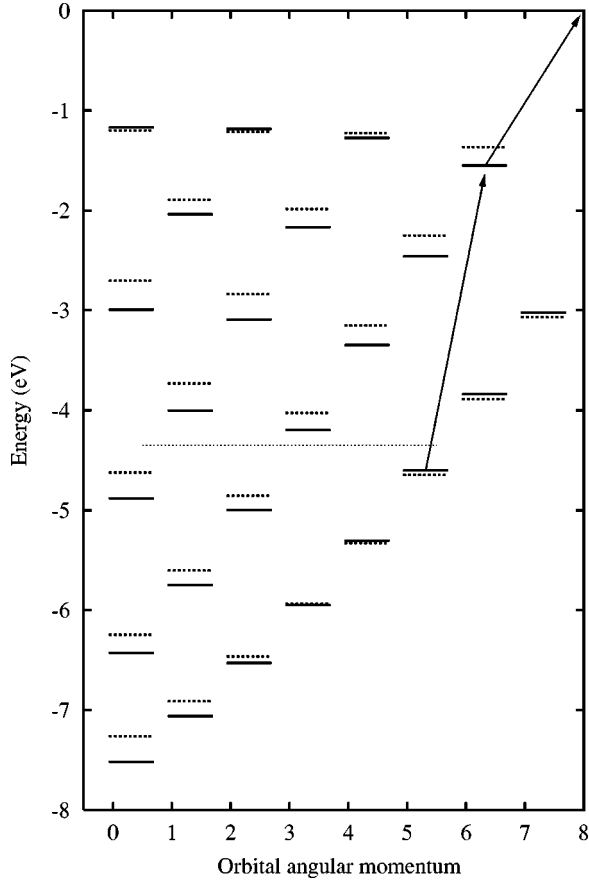


FIG. 1. Single-particle levels in the jellium model of  $\text{Na}_{93}^+$ . The solid and dashed lines correspond to the self-consistent potential and the fitted potential of Eq. (1), respectively. The Fermi level is indicated with a dotted line. The arrows show a two-step transition with a particularly small matrix element in Eq. (16).

a clearer insight into the analytical expressions that we will derive we adopted a more schematic approach where the interaction between electrons is assumed to have a separable form. Such a form has been successfully used in atomic nuclei to study qualitative effects of two-body correlations [8]. It has also been justified in clusters in Ref. [9] where the equivalence between the vibrating potential model and the separable RPA was shown. Thus, we take the residual interaction between electrons to be

$$v(\mathbf{r}, \mathbf{r}') = \kappa \mathbf{f}(\mathbf{r}) \cdot \mathbf{f}(\mathbf{r}'), \quad (3)$$

where  $\mathbf{f}$  is a three-dimensional vector with components  $\mathbf{f}_\mu(\mathbf{r}) \equiv f(r) Y_\mu^\mu(\hat{r})$ . Then, the energies of the RPA excitations satisfy the dispersion relation

$$1 = 2\kappa \sum_{ph} \frac{\langle p | \mathbf{f}_\mu | h \rangle^2 (\epsilon_p - \epsilon_h)}{\omega_n^2 - (\epsilon_p - \epsilon_h)^2}, \quad (4)$$

where  $\epsilon$  is a single-particle energy and  $p, h$  label particle and hole orbitals. In the study of electron emission by plasmons the correct value of the plasmon energy is of crucial importance. It is known that in standard jellium RPA models the plasmon energy is overestimated. In our separable model  $\kappa$

will be used as a parameter adjusted to reproduce the empirical plasmon energy. Due to the spherical symmetry, the solutions  $\omega_n$  of the dispersion relation are independent of  $\mu$ .

The matrix element  $\langle n\mu | \mathbf{f}_\mu | 0 \rangle$  between the ground state and a one-plasmon state of energy  $\omega_n$  will be needed in the following. In our simple model it is given by

$$\langle n\mu | \mathbf{f}_\mu | 0 \rangle = \frac{1}{2\kappa} \left( \omega_n \sum_{ph} \frac{\langle p | \mathbf{f}_\mu | h \rangle^2 (\epsilon_p - \epsilon_h)}{[\omega_n^2 - (\epsilon_p - \epsilon_h)^2]} \right)^{-1/2}. \quad (5)$$

In the spherical jellium model, the surface plasmon can be roughly described taking the interaction of dipole-dipole form [9]. For an excitation along the  $z$  axis, the field is  $z$ , i.e., a radial field of the form

$$f(r) = r. \quad (6)$$

Using Eq. (4) and the experimental value  $\omega_n = 2.75$  eV we obtain  $\kappa = 0.91 \times 10^{-2}$  eV  $\text{\AA}^{-2}$ .

Note that, if one assumes that the transition density  $\delta\rho_{n\mu}(\mathbf{r}) \equiv \langle n\mu | \sum_i \delta(\mathbf{r} - \mathbf{r}_i) | 0 \rangle$  of the plasmon is concentrated at the surface at radius  $R$ , the strength of the interaction is obtained from the multipole expansion of the Coulomb interaction as

$$\kappa_c = \frac{e^2}{R^3}. \quad (7)$$

The dispersion relation can then be solved analytically [10] in the limit  $\omega_n \gg (\epsilon_p - \epsilon_h)$  making use of the TRK sum rule. The result is the simple Mie surface plasmon formula,

$$\omega_n^2 = \frac{e^2 \hbar^2 N}{m R^3}. \quad (8)$$

The resulting energy is about 25% higher than the empirical value for sodium clusters,  $\omega_n \approx 2.75$  eV. One can see that our coupling strength is  $0.52\kappa_c$ .

In the ionization calculation a quantity of particular importance is the transition potential defined as

$$v_{n\mu}(\mathbf{r}) \equiv \int v(\mathbf{r}, \mathbf{r}') \delta\rho_{n\mu}(\mathbf{r}') d^3 r'. \quad (9)$$

For our separable interaction it is given by

$$v_{n\mu}(\mathbf{r}) = \kappa \mathbf{f}_\mu(\mathbf{r}) \langle n\mu | \mathbf{f}_\mu | 0 \rangle. \quad (10)$$

However, the transition potential of Eq. (10) calculated with Eq. (6) is linear in  $r$  whereas TDLDA calculations without separable assumption do not yield this behavior, as shown in Fig. 2. A simple improvement over the linear form Eq. (6) is the dipole field associated with a charge distribution localized on the surface of the jellium sphere [11]. A surface charge produces a radial field of the form

$$f(r) = \begin{cases} r & r < R, \\ \frac{R^3}{r^2} & r > R. \end{cases} \quad (11)$$

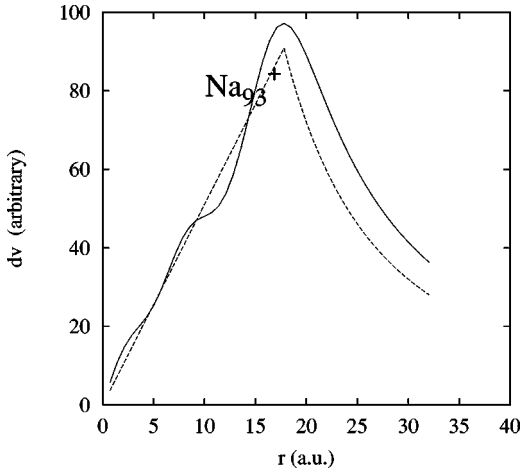


FIG. 2. Transition potential, comparing full RPA with Eqs. (10), (11).

This is plotted as the dashed line in Fig. 2; it clearly is much closer to the actual TDLDA transition potential. With this choice, the empirical position of the resonance is obtained by increasing the coupling constant by about 10%. This shows that the modified form factor has only a small influence on the plasmon properties which are related to bound electron orbitals. However, for matrix elements containing unbound electron states such as those involved in electron emission the differences between the two form factors are much more important as we will see in the next section.

The photoabsorption cross section  $\sigma(\omega)$  which is known experimentally [12] is related to the dynamic polarizability  $\alpha(\omega)$  by

$$\sigma = 4\pi \frac{\omega}{\hbar c} \text{Im } \alpha(\omega), \quad (12)$$

where the dynamic polarizability is

$$\alpha(\omega) = \sum_n \frac{2e^2 \langle n|z|0\rangle^2 \omega_n}{\omega_n^2 - (\omega - i\delta)^2}. \quad (13)$$

Here,  $n$  labels the true excitations and  $i\delta$  is an imaginary quantity. The experimental photo-absorption spectrum has a width of about 0.5 eV. This finite width requires theory beyond RPA, which produces only zero-width excitations below the ionization threshold. Since it is not easy to incorporate the other degrees of freedom that are responsible for the width, it will be treated phenomenologically. Taking a single pole approximation for the plasmon in Eq. (13) and replacing  $\delta$  by  $\Gamma_n/2$  where  $\Gamma_n$  is the width of the photoabsorption peak we obtain the dotted curve of Fig. 3 for  $\text{Im } \alpha(\omega)$ . This is compared in the same figure to the result of Eq. (12) using the experimental cross section. In a realistic RPA the photoabsorption peak is fragmented into several states and the external width parameter needed to reproduce the experimental spectrum is therefore smaller. This is seen in Fig. 3 where the full RPA response for the soft jellium model we show [13] (i.e., with a soft-edged surface in the distribution of the background charge) calculated using the program JELLYRPA.

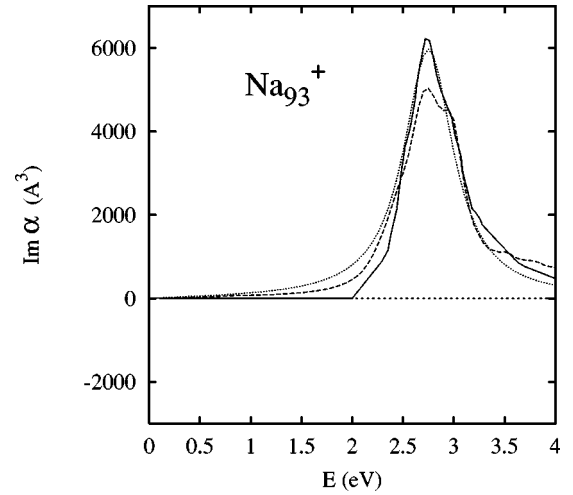


FIG. 3. Imaginary part of the dynamic polarizability of  $\text{Na}_{93}^+$ : empirical from Ref. [12] and Eq. (12) (solid line); single-pole approximation (dotted line); RPA with soft jellium model (dashed line).

In this case the empirical width can be reproduced with  $\Gamma_n = 0.3$  eV. Both these models give a reasonable but not quantitative description of the data. The soft jellium model has the advantage that the plasmon can be moved to lower frequency without adjusting the coupling strength. However, it predicts too low an ionization potential, which makes it unsuitable for the autoionization calculation.

### III. TWO-PLASMON AUTOIONIZATION RATE

The ionization width  $\Gamma_e = \hbar w_e$ , where  $w_e$  is the ionization rate, is given by the Golden Rule formula

$$\Gamma_e = 2\pi \sum_{ph} |M_{ph}|^2 \frac{dn_p}{dE} \delta(2\omega_n - \epsilon_p + \epsilon_h), \quad (14)$$

where one has to integrate over the emitted electron energy  $\epsilon_p$  and where  $dn_p/dE$  is the density of states of the continuum electron. The many-body lowest order perturbative graphs for  $M_{ph}$ , the interaction matrix element between the two-plasmon excitation of the  $n\mu$  mode and the final configuration with a hole  $h$  and the electron in a continuum state  $p$ , is shown in Fig. 4. The labels  $p', h'$  stand for particle and hole states, respectively. Algebraically, the matrix element is given by

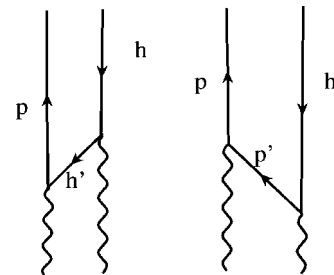


FIG. 4. Perturbation theory graphs for second-order ionization.

$$\begin{aligned}
M_{ph} &= \sqrt{2} \left[ \sum_{p'} \left( \frac{\langle h|v_{n\mu}|p'\rangle \langle p'|v_{n\mu}|p\rangle}{\omega_n - \epsilon_{p'} + \epsilon_h} \right) \right. \\
&\quad \left. - \sum_{h'} \left( \frac{\langle h|v_{n\mu}|h'\rangle \langle h'|v_{n\mu}|p\rangle}{\omega_n - \epsilon_{p'} + \epsilon_{h'}} \right) \right] \\
&= \sqrt{2} \sum_{i'} \left( \frac{\langle h|v_{n\mu}|i'\rangle \langle i'|v_{n\mu}|p\rangle}{\omega_n - \epsilon_{i'} + \epsilon_h} \right), \quad (15)
\end{aligned}$$

where  $v_{n\mu}$  is defined in Eq. (9). The factor  $\sqrt{2}$  accounts for the statistics of the two-plasmon initial state. The two graphs can be combined in one sum over both particles and holes as shown in the second line, making use of the fact that the matrix element is only required on shell, i.e., with  $\epsilon_p - \epsilon_h = 2\omega_n$ . The primed indices  $i'$  indicate particle or hole orbitals, depending on the direction of the arrow.

For our separable interaction Eq. (3) the plasmon term can be separated out and the width  $\Gamma_e$  becomes

$$\Gamma_e = 4\pi\kappa^4 \langle n|\mathbf{f}_\mu|0\rangle^4 \sum_{ph} |K_{ph}|^2 \frac{dn_p}{dE} \delta(2\omega_n - \epsilon_p + \epsilon_h), \quad (16)$$

where  $K_{ph}$  is given by

$$K_{ph} = \sum_{i'} \left( \frac{\langle h|\mathbf{f}_\mu|i'\rangle \langle i'|\mathbf{f}_\mu|p\rangle}{\omega_n - \epsilon_{i'} + \epsilon_h} \right). \quad (17)$$

The sums in Eq. (14) can be reduced in size by making use of the angular momentum symmetry of the orbitals. Labeling the angular momentum quantum numbers  $l$  and  $m$ , we may express the  $m$  dependence of the matrix elements as

$$\begin{aligned}
\langle p', m_{p'} | \mathbf{f}_\mu | p, m_p \rangle &= (-1)^{l_{p'} - m_{p'}} \begin{pmatrix} l_{p'} & 1 & l_p \\ -m_{p'} & \mu & m_p \end{pmatrix} \\
&\quad \times \langle p' || \mathbf{f} || p \rangle, \quad (18)
\end{aligned}$$

where the reduced matrix element  $\langle a || \mathbf{f} || b \rangle$  is defined as [14]

$$\begin{aligned}
\langle a || \mathbf{f} || b \rangle &= (-1)^{l_a} \sqrt{(2l_a + 1)(2l_b + 1)} \begin{pmatrix} l_a & 1 & l_b \\ 0 & 0 & 0 \end{pmatrix} \\
&\quad \times \int_0^\infty f(r) \varphi_a(r) \varphi_b(r) r^2 dr \quad (19)
\end{aligned}$$

in terms of the radial wave functions  $\varphi_i$ . The sum over magnetic quantum numbers  $m_{p,h}$  implicit in Eq. (14) can be evaluated in terms of a 9- $j$  symbol [15] in which the total angular momentum  $L$  carried by the two photons appears. The result is

TABLE I. Two-plasmon ionization widths in  $\text{Na}_{93}^+$ . The quantities  $\tau_e$  are the corresponding lifetimes.

$f(r) = r$ $\kappa = 0.91 \times 10^{-2} \text{ eV } \text{\AA}^{-2}$			
$\delta(\text{eV})$	0.0	0.1	0.2
$\Gamma_e(\text{eV})$	$9 \times 10^{-4}$	$5 \times 10^{-4}$	$4 \times 10^{-4}$
$\tau_e(\text{fs})$	$7.3 \times 10^2$	$13.2 \times 10^2$	$16.5 \times 10^2$
$f(r)$ of Eq. (11) $\kappa = 1.03 \times 10^{-2} \text{ eV } \text{\AA}^{-2}$			
$\delta(\text{eV})$	0.0	0.1	0.2
$\Gamma_e(\text{eV})$	$8.8 \times 10^{-2}$	$5.5 \times 10^{-2}$	$3.8 \times 10^{-2}$
$\tau_e(\text{fs})$	7.5	12.0	17.4

$$\begin{aligned}
\sum_{\text{all } m} |K_{ph}|^2 &= 2 \sum_{ij} \frac{1}{[\omega_n - (\epsilon_j - \epsilon_h)][\omega_n - (\epsilon_i - \epsilon_h)]} \langle h || \mathbf{f} || j \rangle \\
&\quad \times \langle j || \mathbf{f} || p \rangle \langle p || \mathbf{f} || i \rangle \langle i || \mathbf{f} || h \rangle \sum_{L=0,2} (2L+1) \\
&\quad \times \begin{pmatrix} 1 & 1 & L \\ 0 & 0 & 0 \end{pmatrix}^2 \begin{Bmatrix} 1 & 1 & L \\ l_j & l_p & 1 \\ l_h & l_i & 1 \end{Bmatrix}. \quad (20)
\end{aligned}$$

The factor of 2 arises from the two-fold spin degeneracy of the occupied orbitals. In carrying out the calculation one also has to fix the normalization of the continuum radial wave function. A convenient choice is  $r\varphi_p \rightarrow \sin(kr + \delta)$  at large  $r$ , giving  $dn_p/dE = 2m/(\pi k \hbar^2)$ .

As always in perturbative expressions the denominators in Eq. (20) can be very small for some  $i$  or  $j$  states. The standard procedure to avoid unphysically large contributions is to introduce an imaginary part  $i\delta$  which represents the combined width of initial and final states. This width cannot be precisely determined but a way to choose it is to look for a range of  $\delta$  where  $K_{ph}$  is stable.

The results for the autoionization of  $\text{Na}_{93}^+$  are given in Table I for the two choices of separable force, Eqs. (6) and (11), in the upper and lower part of the table, respectively. One can see a strong dependence of the results on the choice of  $f(r)$ . We recall that the choice of Eq. (11) gives the closest agreement for the plasmon transition potential as compared with the full RPA calculation. The introduction of the width  $\delta$  reduces the ionization width  $\Gamma_e$  but the dependence of the results seems moderate in the range  $\delta \approx 0.1 - 0.2 \text{ eV}$ . This is also illustrated in Fig. 5.

With the choice of Eq. (11) the calculated ionization lifetime  $\tau_e$  of the two-plasmon state is in the range of 10 to 20 fs. This is of the same order of magnitude as, or larger than the plasmon lifetime which is estimated to be about 10 fs [2]. Within the uncertainties of our model it seems that the ionization process could compete with the plasmon damping but with a small branching ratio. In any case the ionization process is not very fast contrarily to the assumption made in Ref. [2]. On the other hand, if one considers the choice of

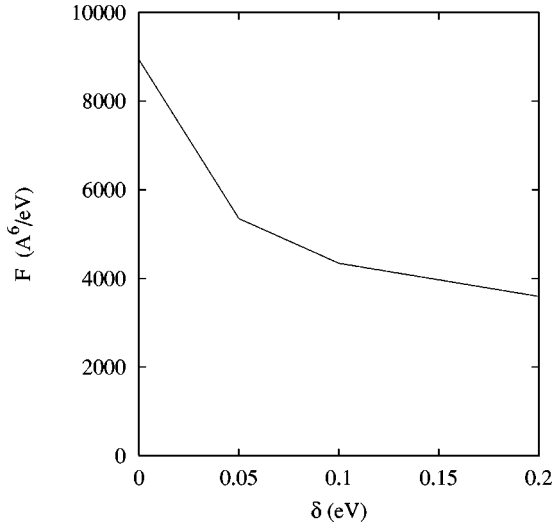


FIG. 5. Second-order term  $\pi e^4/2|K^{(2)}|^2 dn_p/dE$  as a function of  $\delta$ .

Eq. (6) the direct ionization process is still slower and most of the observed electrons should not come from a direct emission. A recent analysis of the same experiment [16] seems to indicate indeed that the observed electrons have a statistical spectrum.

#### IV. IONIZATION IN A LASER FIELD

In this section we wish to apply the previous results to ionization in a laser field. Thus, we consider the ionization as a multistep process, in which the photons are first absorbed to make plasmons and then the plasmons interact to eject an electron. A simple physical argument can be made to obtain a formula for the ionization. Let us define the absorption rate for photons  $R_\nu$  and the damping width for the plasmon  $\Gamma_n$ . In the steady state the balance between the creation and absorption of plasmons gives a mean number of plasmons  $\bar{n}$  satisfying

$$\bar{n} = \frac{\hbar R_\nu}{\Gamma_n}. \quad (21)$$

Taking the distribution of numbers as Poissonian, the mean number of pairs is then  $\bar{n}^2/2$ . The ionization rate  $R_e$  is related to the two-plasmon ionization width  $\Gamma_e$  by

$$\begin{aligned} R_e &= \frac{\bar{n}^2}{2} w_e \\ &= \frac{\hbar}{2} \frac{R_\nu^2}{\Gamma_n^2} \Gamma_e, \end{aligned} \quad (22)$$

where  $\Gamma_e$  and  $w_e$  have been introduced in the preceding section.

To estimate the probability of direct electron emission it is convenient to define the ratio  $P_e$  of the number of ionizations per cluster,  $N_e = R_e T$ , and the number of pairs of pho-

tons absorbed,  $N_\nu^2/2$  where  $N_\nu = R_\nu T$ ,  $T$  being the time duration of the laser pulse. We thus obtain

$$\begin{aligned} P_e &\equiv \frac{N_e}{N_\nu^2/2} \\ &= \frac{\hbar}{T} \frac{\Gamma_e}{\Gamma_n^2}. \end{aligned} \quad (23)$$

To evaluate the ratio  $P_e$  we take the calculated  $\Gamma_e$  from Sec. III and the experimental pulse duration  $T=140$  fs [2]. As in Sec. II we use for  $\Gamma_n$  the empirical width of the photoabsorption spectrum, 0.5 eV and we obtain for  $P_e$  the values  $1. \times 10^{-5}$  or  $1.1 \times 10^{-3}$  if we take Eq. (6) or (11), respectively. This ratio appears very small even in the more realistic case of Eq. (11). This is in agreement with the recent experimental analysis [16].

#### V. CONCLUSION

In this work, we have studied cluster ionization by two photons of frequency near that of the surface plasmon. The weak coupling between the surface plasmons is the driving interaction for the two-photon ionization process, and a perturbative framework with respect to the ionized electron seems reasonable. First, we have made an evaluation of the direct electron emission by a two-plasmon state in the  $\text{Na}_{93}^+$  cluster. The plasmon is described in a schematic RPA model assuming a separable residual interaction between valence electrons determined so that the experimental properties of the plasmon are reproduced. We find an ionization lifetime of the order of 10–20 fs or larger showing a possible competition between direct ionization and other relaxation processes. Nevertheless, due to the uncertainties of the model the calculated lifetime is not short enough to allow to conclude unambiguously whether direct emission can be observed or not.

With the help of this calculated ionization rate we have estimated in a simple model the number  $P_e$  of emitted electrons per pair of absorbed photons. This ratio is at most  $10^{-3}$  then rather small. The fact that the calculated values of  $P_e$  are small seems compatible with the recent analysis [16] of the experiment of Ref. [2]. Of course, we have used a simple semiempirical RPA based on the jellium model. One could improve the present calculations by replacing the jellium by more refined descriptions of the ionic background [17], and by using more realistic interactions [18]. For small Na clusters, more realistic calculations are becoming available of high field ionization using the TDLDA [19], and it would be interesting to compare our simple approach with these more elaborate calculations.

#### ACKNOWLEDGMENTS

We thank P.G. Reinhard for discussions, and G.B. thanks the IPN at Orsay where this work was done for its hospitality. He was also supported in part by the U.S. Department of Energy under Grant No. DE-FG-06-90ER40561.

- [1] W.A. de Heer, *Rev. Mod. Phys.* **65**, 611 (1993).
- [2] R. Schlipper, R. Kusche, B. von Issendorff, and H. Haberland, *Phys. Rev. Lett.* **80**, 1194 (1998).
- [3] G. Senatore and K.S. Subbaswamy, *Phys. Rev. A* **35**, 2440 (1987).
- [4] X. Tong and S. Chu, *Phys. Rev. A* **57**, 452 (1998).
- [5] C.A. Ullrich and E.K.U. Gross, *Comments At. Mol. Phys.* **33**, 211 (1997).
- [6] C.A. Ullrich, P.G. Reinhard, and E. Surraud, *J. Phys. B* **30**, 5043 (1997).
- [7] G.F. Bertsch, *Comput. Phys. Commun.* **60**, 247 (1990).
- [8] A. Bohr and B.R. Mottelson, *Nuclear Structure* (Benjamin, Reading, 1975), Vol. II, Eq. (6-37).
- [9] E. Lipparini and S. Stringari, *Z. Phys. D* **18**, 193 (1991).
- [10] G.F. Bertsch and R.A. Broglia, *Oscillations in Finite Quantum Systems* (Cambridge, New York, 1994), p. 86.
- [11] K. Yabana and G.F. Bertsch, *Z. Phys. D* **32**, 329 (1995).
- [12] T. Reiners, *et al.* *Phys. Rev. Lett.* **74**, 1558 (1995).
- [13] F. Calvayrac, E. Surraud, and P.G. Reinhard, *Ann. Phys. (N.Y.)* **254**, 125 (1997).
- [14] A. Bohr and B.R. Mottelson, *Nuclear Structure* (Benjamin, New York, 1969), Vol. I, p. 82.
- [15] M. Rotenberg *et al.*, *The 3-j and 6-j Symbols* (MIT Press, Cambridge, MA, 1959), Eq. (1.22-24).
- [16] H. Haberland and B. von Issendorff (private communication).
- [17] K. Yabana and G.F. Bertsch, *Phys. Rev. B* **54**, 4484 (1996).
- [18] M. Madjet, C. Guet, and W.R. Johnson, *Phys. Rev. A* **51**, 1327 (1995).
- [19] P.G. Reinhard and E. Surraud, *J. Cluster Sci.* **10**, 239 (1999).